Structural and Optical Properties of nc-a TiO_2 films for Dye Sensitized Solar Cell

M.T. SARODE[1], Y. B. KHOLLAM[2], S. D. GUNJAL[3], P.N. SHELKE[4], B. B. KALE[5], K. C. MOHITE[3]

[1] Mahatma Phule A.S.C. College, Panvel, 410 206, India.
[2] Department of Physics, Anantrao Pawar College, Pune 412 115, India.
[3] Department of Physics, H.V. Desai College, Pune 411 007, India.
[4] Department of Physics, Baburaoji Gholap College, Sangvi, Pune 411 027, India.
[5] Center for Materials for Electronics Technology, Panchwati, Pashan, Pune 411 008, India.
Email: sarodemadhav@gmail.com

Abstract

Nanocrystalline anatase (nc-a) TiO_2 films are prepared by using the sol-gel dip-coating processing followed by annealing between 200 - 500 °C for 2 hr in air. The structural studies using XRD and Raman spectroscopy indicated the evolution of pure anatase TiO_2 phase (crystallite size = 12 - 15 nm) in resultant films. The morphological studies with SEM and TEM indicated nanocrystalline state of films. The annealing temperature is noted to have profound effect on optical properties. The structural and optical properties obtained for the resultant films showed an expediency of these films for potential application of photo electrode for dye sensitized solar cells.

Keywords: Nanocrystalline , Anatase TiO_2, Thin films, Optical properties.

Introduction

Nanocrystalline anatase (nc-a) TiO_2 is applied to dye-sensitized solar cells (DSSC) as the material of porous films since the landmark paper [1]. DSSC have been studied extensively because of their high efficiency and low-cost. The highest energy conversion efficiency [2] of DSSCs is 11.04 %. The performance of DSSC depends on the nature of films including crystalline phase [3 - 4] and size of particles. For instance, the short-circuit photocurrent for rutile TiO_2 - based DSSC is about 30 % lower than that of the anatase TiO_2 based DSSC [3 - 4]. Further, the electron transport is slower in rutile layer than in the anatase layer due to different inter-particle connectivity associated with particle packing density. Moreover, for various applications, the size of particles is an important parameter because it determines the surface to volume ratio greatly influencing many factors. The optimal TiO_2 particle sizes for DSSC are approximately 10 - 25 nm [2, 5 - 6]. The anatase and rutile TiO_2 can be obtained when pH of the autoclaving solution varies from 0.8 to 1.5 at 230 - 270 ^{0}C [7]. This synthesis method has attracted more attention in the preparation of porous nc-TiO_2 thin films applied to DSSC.

In this paper, preparation of nc-anatase (nc-a) TiO_2 films by using sol-gel dip coating technique is reported. The resultant nc-a TiO_2 films were characterized by using XRD, Raman spectroscopy, SEM and TEM. The optical properties of resultant nc-a TiO_2 films were obtained by using UV-visible spectroscopy studies.

Materials and Methods

A 4.05 ml of titanium tetra-isopropoxide (TTIP) was added slowly to 11.25 ml of double distilled water (DDW) [molar ratio of Ti: H_2O = 0.1:5.0] at room temperature (RT) under vigorous stirring for 2 h. The detail procedure for the preparation of nc-a TiO_2 films on glass substrate is given in our earlier report [8].

Results and Discussion

Fig. 1 (a) gives the XRD patterns for resultant films. The 200 ^{0}C annealed film shows the amorphous nature. The evolution of phase is started at 300 ^{0}C.

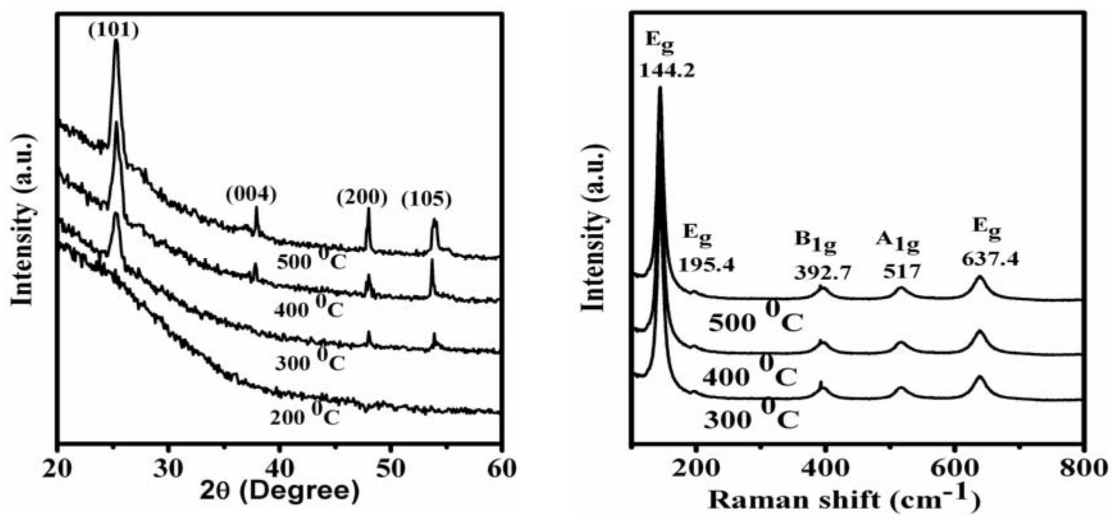

(a) (b)

Fig. 1. (a) XRD patterns and (b) Raman spectra of resultant films

All the reflections in the XRD patterns for 300, 400 and 500 ^{0}C annealed films are found to be matching with the peaks for pure anatase TiO_2 [JCPDS file No. 21-1272] only indicating thereby single phase nature of film materials. The data for lattice parameters [9] and interplaner spacing d_{101} obtained are summarized in Table I. The observed values are approximately equals with standard values given in literature [a = b = 0.3730 nm, c = 0.9485 nm & d = 0.3520 nm] [JCPDS file No. 21-1272]. The values average crystallite size (D) obtained by using Scherrer [10] relation:

$$D = (0.9\lambda/\beta\cos\theta)$$

[λ = 0.1541 nm, β = FWHM, θ = diffraction angle] for all films are found to in nanometric range.

The crystallite size is found to be increasing with annealing temperature. The Raman spectra for resultant films given in Fig. 1 (b) show well defined peaks and the absence of overlapping peaks. The spectra show well crystallized nature of all films with less number of imperfect sites. All spectra show

5 Raman active bands centered at 144.2 cm^{-1} (E_g), 195.4 cm^{-1} (E_g), 392.7 cm^{-1} (B_{1g}), 517 cm^{-1} (A_{1g}) and 637.4 cm^{-1} (E_g), which are matching with bands given for single crystal anatase TiO_2 [11]. It confirms the single anatase phase nature of TiO_2 films [12]. This is consistent with XRD results. Fig. 2 shows the SEM images of films annealed at 300, 400 and 500 ^{0}C. The SEM images show the following observations: (i) particles are nearly spherical, (ii) particle size distribution is uniform, (ii) nature of particles is soft agglomerate, (iv) each spherical agglomerate contains many particles in nanometric range and (v) the agglomerate size is in range of 100 - 250 nm. The agglomerate size is consistent with the XRD results for average crystallite size. The images also reveal the porous/less densification nature of the film at the surface. The voids are clearly seen at the surface of the films in the form of cracks. With increasing the heating temperature, the particle size is found to be increasing slightly resulting into the dense agglomeration nature of particles at 400 ^{0}C annealed film.

Table - I

STRUCTURAL PROPERTIES OF RESULTANT FILMS

Temp. (^{o}C)	Crystallite size (nm)	d_{101} spacing (nm)		Phase symmetry	Lattice parameter (nm)			Unit cell volume $(nm)^3$
		Obs.	Std.		a	b	c	
200	--	--	--	Amorphous	--	--	--	--
300	11.97	0.3517	0.3520	Anatase	0.3778	0.3778	0.9497	0.1356
400	13.94	0.3518	0.3520	Anatase	0.3775	0.3775	0.9491	0.1353
500	15.01	0.3517	0.3520	Anatase	0.3771	0.3771	0.9489	0.1349

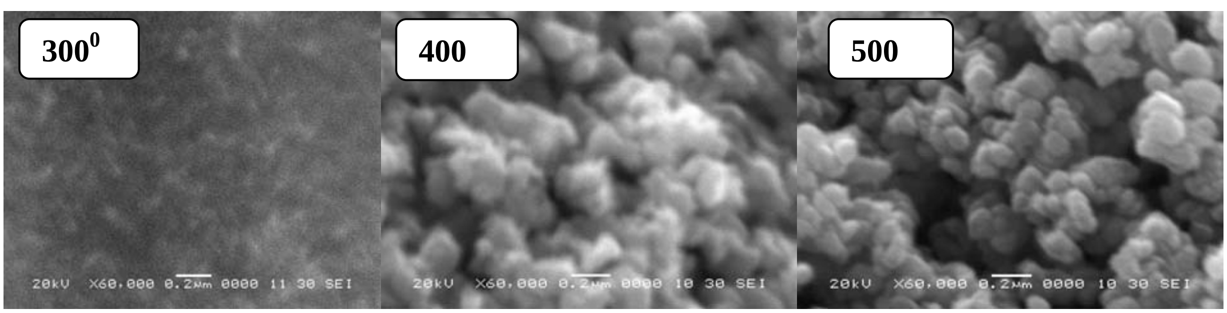

Fig. 2. SEM images of films annealed at 300, 400 and 500 ^{0}C

The high resolution TEM photograph for films annealed at 500 ^{0}C is given in fig. 3. It shows and confirms the nanocrystalline nature of the material of film. Fig. 4 (a) gives UV-Visible % transmittance spectra for the resultant films. The thickness of film (d) is found to be decreasing with increasing the annealing temperature as is expected. This is might be due to the densification of films at higher annealing temperature. The film annealed at 400 ^{0}C exhibit high % T ~ 90 % at 675 nm. The absorption coefficient, (α) = ln(1/T)/d [where, T = % transmittance, d = thickness] is noted to be between 7.57 -

8.03 x 10^4 cm^{-1}. Fig. 4 (b) gives the Tauc's plots [13] of indirect band gaps (E_g) for the resultant films. The value of indirect E_g is obtained by extrapolation of straight-line portion of the plot to zero absorption edge. From Tauc's plots, it is noted that the band-to-band indirect transitions are most probable than the direct transitions for TiO_2 films.

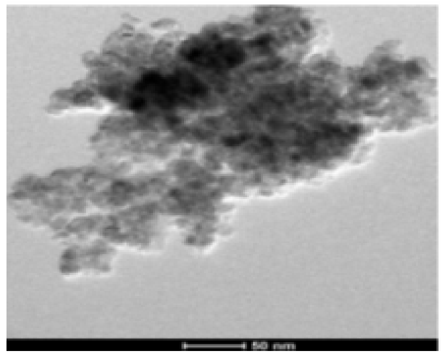

Fig. 3. TEM images of films annealed at 500 ^{0}C

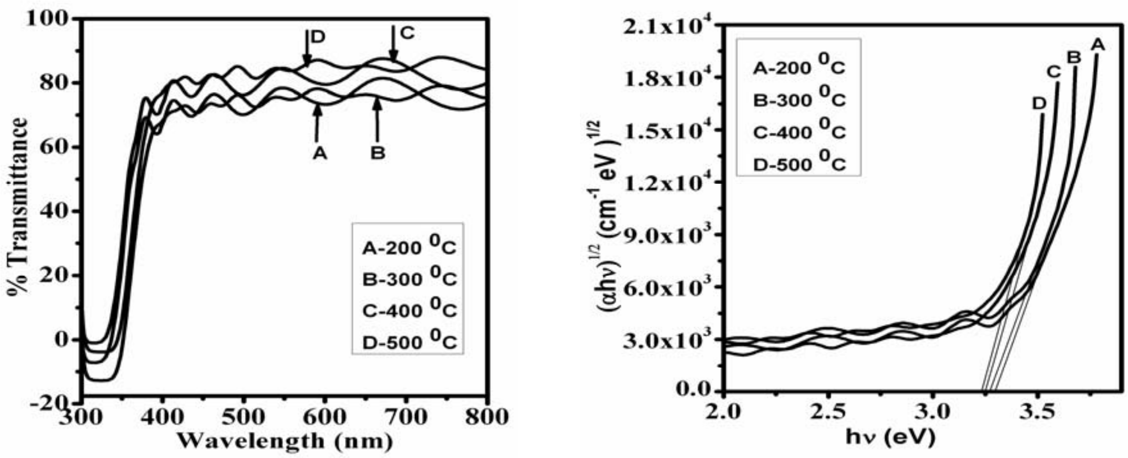

(a) (b)

Fig. 4. (a) UV- Visible transmittance, (b) variation of $(\alpha h\nu)^{1/2}$ vs. hν (indirect band gap) for the resultant films

The band gap is noted to be decreasing with increasing the annealing temperature i.e. with increasing the thickness of films. This is might be due to the increasing the particles size with the annealing temperature. The refractive index (n) of the films calculated by using modified envelope method [14] at λ = 675 nm and is found to be increasing with increasing the annealing temperature.

The optical conductivity (σ_{opt}) [15] of film is also found to be increasing with increasing the annealing temperature. The porosity (% p) [16] of the films depends on the refractivity of the film layer. The porosity obtained by using the refractive index at λ = 675 nm is found to be decreasing with increasing the annealing temperature. This is due to densification of film material at higher temperature i.e.

decreasing the film thickness. The optical properties obtained are summarized in Table 2.

Table 2 Optical Properties Of Resultant Films

Temp. (^{o}C)	d (nm)	% T at λ = 675 nm	Abs. coeff. (α) x 10^{4} (cm^{-1})	indirect E_g (eV)	R.I. (n) at λ = 675 nm	$\sigma_{opt.}$ x 10^{15} s^{-1}	% P
200	586	84.87	7.57	3.30	2.08	6.02	38.98
300	576	78.09	7.58	3.27	2.09	6.04	38.22
400	568	90.22	7.93	3.25	2.09	6.33	38.22
500	558	88.42	8.03	3.22	2.10	6.44	37.45

Conclusions

The sol-gel dip-coating is simple, cheap and versatile processing route useful for the preparation of nanocrystalline anatase TiO_2 films. The structural and morphological studies of resultant films confirmed the phase pure nanocrystalline state of materials of TiO_2 films. The optical properties are found to be influenced by annealing temperature. Hence, these films might be having good potential for the application like photo electrode for dye sensitized solar cells.

Acknowledgment

The author MTS is thankful to Principal Dr. Sanjay Kamble, M.P.A.S.C. College, Panvel, India, Director, School of Energy Studies, Savitribai Phule Pune University, Pune, India and Centre for materials for Electronics Technology (C-MET), Pune, providing research facilities for the present work.

References

[1] B. O’Regan, and M. Grätzel, Nature, 353, 737 (1991).
[2] M. Grätzel, J. Photochem. & Photobiology A: Chemistry, 164, 3 (2004).
[3] M. Koelsch, S. Cassaignon, C. T. T. Minh, J. F. Guillemoles and J. P. Jolivet, Thin Solid Films, 452, 86 (2004).
[4] N. G. Park, G. Schlichthörl, J. Van de Lagemaat, H. M. Cheong, A. Mascarenhas, and A. J. Frank, J. of Phy. Chem. B, 103, 3308 (1999).
[5] M. K. Nazeeruddin, A. Kay, I. Rodicio, R. Humphry-Baker, E. Muller, P. Liska, N. Vlachopoulos, and M. Grätzel, J. Amer. Chem. Soc., 115, 6382 (1993) .
[6] Z.-S. Wang, T. Yamaguchi, H. Sugihara and H. Arakawa, Langmuir, 21, 4272 (2005).
[7] M. T. Sarode, P. N. Shelke, Y. B. Khollam, M. G. Takwale, S. R. Jadkar, B. B. Kale and K. C. Mohite, Inter. J. Modern Phys. B, 25 (31), 4163 (2011).
[8] B. Yarmand and S. K. Sadrnezhaad, J. Optoelectronics & Adv. Mater., 12 (7), 1490 (2010).
[9] B. D. Cullity, Elements of X-ray diffraction, (Wesley Publishing Company Inc., London, 1978).
[10] T. Ohsaka, Y. Izumi and Y. Fujiki, J. Raman Spectroscopy, 7, 321 (1978).

[11] R. Mechiakh, N. B. Sedrine, J. Ben Naceur and R. Chtourou, Surface & Coatings Tech. (In press).

[12] P. Chrysicopoulou, D. Davazoglou, C. Trapalis, and G. Kordas, Thin Solid Films, 323, 188 (1998).

[13] S. Sankar and K. G. Gopchandran, Cryst. Res. Technol., 44, 989 (2009).

[14] D. B. Williams and C. Barry Carter, A textbook for Materials Science (Plenum Publishing Corpn.,) (1996).

[15] M. M. Hasan, A. S. M. A. Haseeb, R. Saidur and H. H. Masjuki, Inter. J. Chem. Bio. Engg., 1, 97 (2008).